

Electric field effect modulation of transition temperature, mobile carrier density and in-plane penetration depth in $\text{NdBa}_2\text{Cu}_3\text{O}_{7-\delta}$ thin films

D. Matthey,* N. Reyren, and J.-M. Triscone

DPMC, University of Geneva, 24 quai Ernest-Ansermet, 1211 Geneva 4, Switzerland.

T. Schneider

Physikinstitut, University of Zurich, Winterthurerstrasse 190, 8057 Zurich, Switzerland.

(Dated: May 25, 2019)

We explore the relationship between the critical temperature, T_c , the mobile areal carrier density, n_{2D} , and the zero temperature magnetic in-plane penetration depth, $\lambda_{ab}(0)$, in very thin underdoped $\text{NdBa}_2\text{Cu}_3\text{O}_{7-\delta}$ films near the quantum superconductor to insulator (QSI) transition using the electric field effect technique. We observe that T_c depends linearly on both, n_{2D} and $1/\lambda_{ab}^2(0)$, signifying the occurrence of a QSI transition in 2D, occurring in superconducting sheets of thickness $d_s \simeq 9\text{\AA}$.

PACS numbers: 71.30.+h, 74.78.Bz, 74.72.-h, 74.75.Ha

The electronic properties of high T_c superconductors are critically determined by the density of mobile holes as illustrated by their generic phase diagram in the temperature dopant concentration plane. Understanding the physics of this phase diagram, in particular at the two $T = 0$ edges of the superconducting dome, has emerged as one of the critical questions in the field of cuprate superconductors. In the underdoped regime, where the quantum superconductor to insulator (QSI) transition occurs, there is an empirical linear relation between T_c and $\lambda_{ab}^{-2}(0)$ [1], where λ_{ab} is the in-plane London penetration depth. Such a relation holds true when, in the underdoped limit, a two dimensional (2D) QSI-transition occurs [2]. An essential requirement is thus the occurrence of a 3D to 2D crossover as the underdoped limit is approached with a diverging anisotropy $\gamma = \lambda_c/\lambda_{ab}$. Otherwise, the QSI-transition occurs in 3D with $T_c \propto \lambda_{a,b,c}(0)^{-2z/(z+1)}$, where z is the dynamic critical exponent of the transition [2]. Recent penetration depth measurements on $\text{YBa}_2\text{Cu}_3\text{O}_{6+x}$ single crystals [3, 4] (where γ saturates at low doping levels) and films [5] suggest a 3D-transition with $2z/(z+1) \simeq 1$ [6]. We note however that all the studies on the relationship between T_c and $\lambda_{a,b,c}(0)$ are based on data from samples where the doping level was modified by chemical substitution [1, 2, 3, 4, 5, 6, 7, 8].

In this letter we use the electrostatic field effect to tune the mobile areal carrier density, n_{2D} , in ultra-thin, strongly underdoped $\text{NdBa}_2\text{Cu}_3\text{O}_{7-\delta}$ (NBCO) films and explore the intrinsic relation between T_c , n_{2D} and $\lambda_{ab}^{-2}(T=0)$ close to the QSI-transition. The electrostatic field effect technique, which allows the carrier density in a given sample to be changed without affecting the chemical composition, thus avoiding sample to sample variations and substitution induced disorder, appears to be an ideal method to elucidate the intrinsic relationships between the key physical parameters [9].

In a classical oxide field effect configuration, an electric

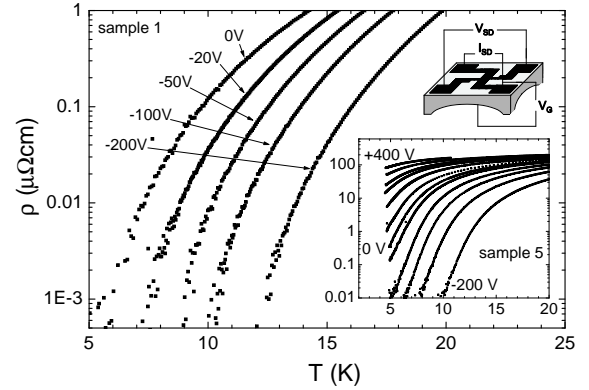


FIG. 1: ρ vs. T for a 3-4 unit cells thick NBCO film (sample 1) for different applied gate voltages. The lower inset shows the resistivity as a function of temperature for sample 5, which is also 3-4 unit cell thick, for different applied gate voltages. The upper inset shows a sketch of the field effect device, based on a thinned STO single crystal gate insulator.

field is applied across a gate dielectric in a heterostructure made of an oxide channel and a dielectric layer. The density of carriers is modified at the interface between the oxide channel and the dielectric, changing the electronic properties of the oxide channel. This technique allows us to induce in thin oxide superconducting films rather large T_c modulations [10]. In the 3-4 unit cells thick films used in this study, T_c , modulations of more than 10 K have been achieved, corresponding to induced charge densities of the order of $0.7 \cdot 10^{14}$ charges/cm². Comparing the electric field effect modulation of the zero temperature (liquid phase) vortex activation energies, U_0 , with the T_c modulations, we demonstrate that in heavily underdoped films, $T_c \propto n_{2D} \propto \lambda_{ab}^{-2}(T=0)$ holds, in agreement with a 2D-QSI-transition, where the film decouples into superconducting sheets of thickness $d_s \simeq 9\text{\AA}$. Furthermore, it is found that in less underdoped samples $dT_c/d(1/\lambda_{ab}^2(0))$ decreases with increasing doping level.

The field effect device used in this study, described in Ref. [10], is based on a STO single crystal gate dielectric, the substrate itself. Due to its large low temperature dielectric constant, ϵ , and large achievable polarizations, STO is a particularly interesting gate insulator. Field effect devices using a STO thin film gate insulator have thus been studied extensively [11]. Here, thin $100\ \mu\text{m}$ thick, or thinned $500\ \mu\text{m}$ commercial substrates have been used. A sketch of the thinned device is shown in the upper inset of Fig.1. The superconducting NBCO thin films are first grown by off-axis magnetron sputtering onto (001) (bare or etched) STO substrates heated to about 730°C . During cooling, a typical O_2 pressure of $670\ \text{Torr}$ is used to obtain optimally doped films. To reduce the doping level, the pressure is lowered down to $5\ \text{mTorr}$. Gold is then sputtered in-situ at room temperature to improve the contact resistances and the whole structure is protected by an amorphous NBCO layer also deposited in-situ. After deposition, the sample is photolithographically patterned using ion milling and a gold electrode is deposited on the backside of the sample, facing the central part of the superconducting path. The thin films studied here are $3 - 4$ unit cells thick.

Fig.1 shows the resistivity of sample 1 as a function of temperature in the tail of the transitions, for different voltages applied across the gate dielectric: $0, -20, -50, -100$ and -200V . Negative voltages correspond to a negative potential applied to the gate and a positive one to the superconducting path, resulting in hole doping of the oxide channel and, as expected, in an increase of T_c . Resistivity measurements are performed using a standard four point technique while a voltage, V_g , is applied to the gate. During measurements, gate leakage currents were kept below a few nA, while the current used for resistivity measurements was typically between 1 and $10\ \mu\text{A}$. The lower inset of Fig.1 shows the resistivity versus temperature for sample 5 and for gate voltages of $400, 200, 100, 50, 20, 10, 0, -5, -20, -50, -100,$ and $-200\ \text{V}$. At 4.2K , a large increase in resistivity is observed while applying positive gate voltages, effectively reducing the hole concentration.

In order to correlate the field-induced T_c modulations to the changes in the field-induced areal carrier density, Δn_{2D} , we measured the accumulated charge. Since the dielectric constant of STO depends on temperature and applied electric field, we measured the field and temperature dependence of the capacitance [12]. The induced areal charge density, $\sigma = e\Delta n_{2D}$, at a given temperature was measured in terms of the capacitance of the device as a function of the applied gate voltage, using an LCR meter (Agilent 4284A) with an auto-balancing bridge method, or by measuring the charge flow during loading using an electrometer (Keithley 6514). The resulting field induced charges, $dQ = C(V)dV$, measured at $4.2\ \text{K}$ are depicted in the inset of Fig.2 for a $100\ \mu\text{m}$ thick STO substrate with two parallel $20\ \text{mm}^2$ square gold elec-

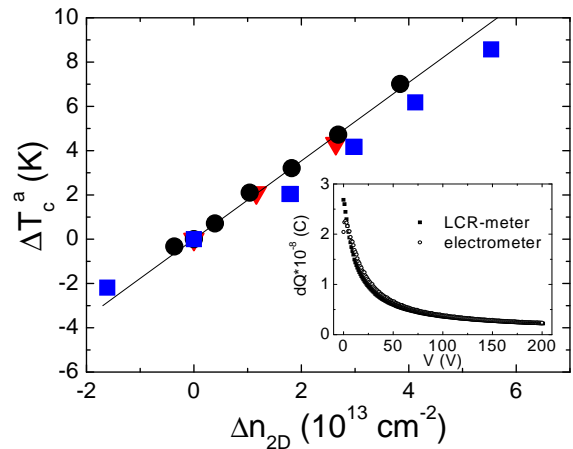


FIG. 2: ΔT_c^a vs. Δn_{2D} for three strongly underdoped samples. Δn_{2D} is measured with a LCR meter at 1kHz . T_c^a is defined as the temperature at which $\rho = 0.5\ \mu\Omega\text{cm}$. The line is Eq.1. The inset shows the field induced charge $dQ = C(V)dV$ measured at $4.2\ \text{K}$ versus voltage V , using an electrometer and a LCR meter on a $100\ \mu\text{m}$ thick STO substrate with two parallel 20mm^2 square gold electrodes.

trodes. By ramping the voltage across the dielectric, the LCR-meter measures the “local” capacitance $C(V)$ at a given voltage, while the electrometer measures dQ for a given change in voltage. It is seen that the two measurements of $dQ(V)$ agree quantitatively. The corresponding field induced charge density $\sigma(V)$ at a given voltage and temperature is then obtained from $\sigma(V) = \int_0^V dQ/S$, where S is the surface of the gate contact. Fig.2 shows the change of the critical temperature, ΔT_c^a , for three different strongly underdoped NBCO thin films, versus the measured field-induced areal charge density, Δn_{2D} . T_c^a is defined as the temperature at which $\rho = 0.5\ \mu\Omega\text{cm}$. At $V_g = 0\text{V}$, $T_c^a = 4.7\text{K}$, $T_c^a = 5.1\text{K}$ and $T_c^a = 5.4\text{K}$ for sample 2 (■), 5 (●) and 6 (▼), respectively. Because ΔT_c is rather insensitive to the T_c criterion (in the tail of the transitions, see Fig.1), the same Δn_{2D} dependence of ΔT_c is obtained for different choices of T_c . As can be seen in Fig.2, the data reveal close to the QSI-transition the intrinsic linear relationship

$$\Delta T_c = 1.75 \cdot 10^{-13} \Delta n_{2D}, \quad (1)$$

where Δn_{2D} is expressed in cm^{-2} [15]. Noting that close to this transition T_c scales as $n_{2D}^{z\bar{\nu}}$, where z is the dynamic and $\bar{\nu}$ the critical exponent of the zero temperature in-plane correlation length, $\xi_{ab} \propto n_{2D}^{-\bar{\nu}}$ [2], Eq.(1) signifies a 2D-QSI-transition with $z\bar{\nu} \simeq 1$, in agreement with theoretical predictions [13, 14].

Since the transition line $T_c(n_{2D})$ ends at the 2D-QSI critical point ($T = 0, n_{2D} = 0$) (which was established in $\text{GdBa}_2\text{Cu}_3\text{O}_{7-\delta}$ films [9]), T_c and $\lambda_{ab}(0)$ are universally related by [2, 16], [17]:

$$T_c = \frac{\Phi_0^2 d_s}{4\pi^2 \mu_0 k_B R \lambda_{ab}^2(0)}. \quad (2)$$

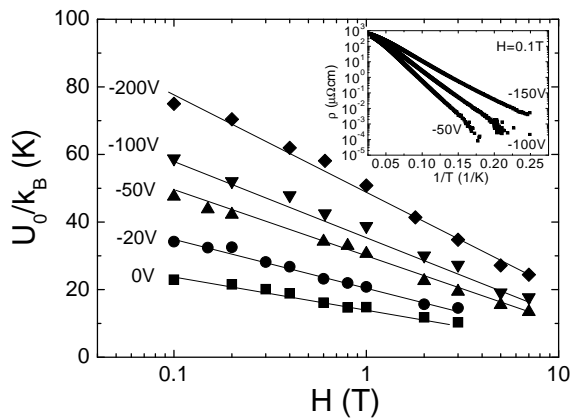


FIG. 3: U_0/k_B vs. H for different applied voltages for sample 1. A linear relation between U_0 and $\log(H)$ is observed with a slope which depends on the applied electrical field. Inset: $\log(\rho)$ as a function of $1/T$ for sample 2 and for three different electrical fields at 0.1T. The zero temperature activation energy U_0 at a given applied electrical field is obtained from the slope of the Arrhenius plot.

R is a universal number most likely around *two* and d_s the thickness of the independent superconducting sheets. This differs drastically from $T_c \propto 1/\lambda_{a,b,c}(0)$, derived from penetration depth measurements on $\text{YBa}_2\text{Cu}_3\text{O}_{6+x}$ single crystals [3, 4] and films [5], where the QSI-transition was tuned by chemical substitution.

Next we explore the relation between T_c and $\lambda_{ab}^{-2}(0)$ close to the field effect tuned 2D-QSI-transition. For this purpose we measured the activation energies, U , for vortex motion in the liquid vortex phase. Noting that the self-energy of a vortex line is proportional to λ^{-2} , one expects $U \propto \lambda^{-2}$ as well. An electric field induced change of λ^{-2} should then modify U . We note that an electrostatic modulation of the activation energies was observed in reference 18. To probe the electric field effect modulation of λ_{ab}^{-2} , we thus measured the magnetic and electric field dependence of U . The magnetic field was applied perpendicular to the ab -plane. The measurements have been performed by ramping the temperature slowly and measuring the sample resistance at a given magnetic and electric field. The inset of Fig.3 shows Arrhenius plots of the resistivity, $\log(\rho)$ as a function of $1/T$, for sample 2 and for three different electrical fields at $H = 0.1\text{T}$. The observed linear relation between $\log(\rho)$ and $1/T$ singles out thermally activated flux flow, where $\rho = \rho_n \exp(-U(H, T)/k_B T)$, with $U(H, T) = 2U_0(H) (1 - T/T_c)$ for $T \sim T_c$ [19, 20, 22]. As can be seen, U becomes larger for electrical fields rising the number of holes and T_c . From such Arrhenius plots we estimated, for sample 1 at different applied voltages, U_0/k_B as depicted in Fig.3 where the U_0/k_B dependence on $\log(H)$ is shown. This logarithmic dependence, observed between 0.1T and 7T, agrees with previous measurements on thin films and superlattices [20, 22] and was

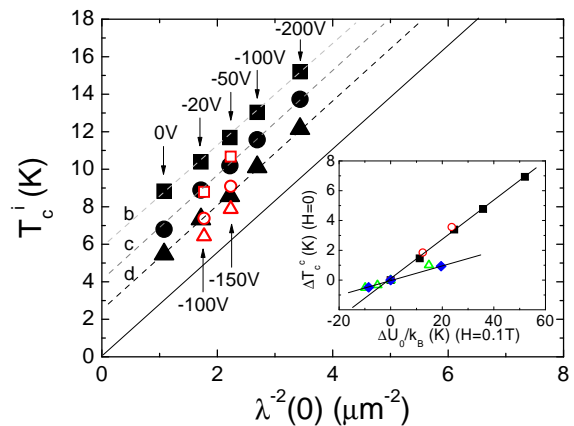


FIG. 4: T_c vs. $1/\lambda^2(0)$ for two strongly underdoped samples, three different T_c estimates and various gate voltages; solid symbols denote sample 1 and open ones sample 2. To demonstrate the approach to the zero resistivity T_c we included the temperatures $T_c^{b,c,d}$ defined respectively as the temperature at which $\rho = 0.05\mu\Omega\text{cm}$ (\blacksquare , \square), $\rho = 0.005\mu\Omega\text{cm}$ (\bullet , \circ), and $\rho = 0.0005\mu\Omega\text{cm}$ (\blacktriangle , \triangle). The full line is Eq.(4) and the dotted ones are guides to the eye. The inset shows ΔT_c^c vs. ΔU_0 taken at 0.1T. Samples 1 (\blacksquare) and 2 (\circ) are strongly underdoped, and samples 3 (\triangle) and 4 (\blacklozenge) are less underdoped. Lines are a guide to the eye.

traced back to a thermally activated dissipation process, associated with the creation of edge dislocation pairs in a 2D vortex structure [20, 21, 22]. In this case, the relation [20, 21]

$$U_0(H) = \frac{\Phi_0^2 d}{16\pi^2 \mu_0 \lambda_{ab}^2(0)} \ln \left(\frac{a_0}{\xi_{ab}(0)} \right), \quad (3)$$

applies, where d is the thickness of the superconducting layer, a_0 the mean vortex-vortex distance and ξ the correlation length. Since, $a_0 = (3\Phi_0/(\sqrt{2}H))^{1/2} \simeq 1.46(\Phi_0/H)^{1/2}$, the magnetic field dependence of the activation energy exhibits the logarithmic field dependence [20], $U_0(H) = -\alpha \ln(H) + \beta$, where $\alpha = \Phi_0^2 d / (32\pi^2 \mu_0 \lambda_{ab}^2(0))$, as confirmed by the data depicted in Fig.3. In the heavily underdoped samples 1 and 2, this $\log(H)$ dependence extends over the full magnetic field range, while in the less underdoped ones, 3 and 4, it is restricted to fields lower than 1T only.

Invoking then Eq.(3) we derived $\lambda_{ab}^{-2}(T=0)$ from the $U_0(H)$ data shown in Fig.3 with $d = 47\text{\AA}$. The resulting estimates, taken at various gate voltages, are plotted in Fig.4 in terms of T_c vs. $\lambda_{ab}^{-2}(0)$. Black symbols refer to sample 1 and open ones to sample 2. To signify the approach to the zero resistivity T_c we included the critical temperatures $T_c^{b,c,d}$ defined respectively as the temperature at which $\rho = 0.05\mu\Omega\text{cm}$ (\blacksquare , \square), $\rho = 0.005\mu\Omega\text{cm}$ (\bullet , \circ), and $\rho = 0.0005\mu\Omega\text{cm}$ (\blacktriangle , \triangle). The data clearly reveal that $T_c \simeq a(T_c^i) + 2.8/\lambda_{ab}^2(0)$, where $a(T_c^i)$ decreases as the zero resistance T_c is approached. Along with that we observe consistency with the universal relation (2),

indicated in Fig. 4 by the straight line, given by

$$T_c = \frac{2.8}{\lambda_{ab}^2(0)}, \quad (4)$$

with $\lambda_{ab}(0)$ in μm . This analysis points again to a 2D-QSI-transition. We note that relation 4 is close to what was obtained in $\text{YBa}_2\text{Cu}_3\text{O}_{7-\delta}$ and $\text{Y}_{1-x}\text{Pr}_x\text{Ba}_2\text{Cu}_3\text{O}_{7-\delta}$ single crystal data with T_c 's ranging from 40 K to 80K [23].

The inset of Fig.4 shows the electrical field effect modulation of the critical temperature ΔT_c^c vs. ΔU_0 for 0.1T. T_c^a at $V_g = 0$ is 12.6K for sample 1, 4.7K for sample 2, 28.5K for sample 3 and 40.4K for sample 4. Samples 1 and 2 are strongly underdoped and samples 3 and 4 less underdoped. It is observed that for a given ΔU_0 the modulation ΔT_c of the strongly underdoped samples is 2.7 times larger. This behavior reveals that $T_c(1/\lambda_{ab}^2(0))$ becomes sublinear with increasing T_c .

Having established the occurrence of a field effect tuned 2D-QSI in thin NBCO films, we are now ready to derive additional relations and estimates between and for characteristic properties. From Eqs.(2) and (4) we obtain $d_s/R \simeq 4.5\text{\AA}$ and with $R \simeq 2$, $d_s \simeq 9\text{\AA}$, compared to the film thickness of 3 to 4 unit cells. This value is close to $d_s \simeq 10\text{\AA}$ derived from the thickness tuned 2D-QSI-transition in $\text{YBa}_2\text{Cu}_3\text{O}_{7-\delta}$ [24]. Consequently, by approaching the 2D-QSI-transition by means of field effect tuning, the thin films decouple into sheets of thickness d_s , while in the chemically tuned case a crossover to a 3D-QSI-transition seems to occur. Furthermore, from Eqs.(1) and (4) we obtain, close to the 2D-QSI-transition, the remarkable relation $n_{2D}\lambda_{ab}^2(0) \simeq 1.6 \cdot 10^{21}$. It implies that isotope or pressure effects on T_c , Δn_{2D} and $\lambda_{ab}(0)$ are not independent. Finally, these results may also strikingly suggest that T_c goes to zero as the system becomes 2-dimensional.

In summary, we explored the relationships between T_c , the mobile areal carrier density, n_{2D} , and the zero temperature in-plane penetration depth, $\lambda_{ab}^2(0)$, for very thin underdoped NBCO films near the quantum superconductor to insulator (QSI) transition by means of the electric field effect technique. We observe a linear relationship between T_c and n_{2D} , as well as evidence for a linear rela-

tionship between T_c and $1/\lambda_{ab}^2(0)$, signifying the occurrence of a QSI-transition in 2D, occurring in decoupled superconducting sheets of thickness $d_s \simeq 9\text{\AA}$.

We would like to thank P. Martinoli and S. Gariglio for useful discussions and M. Dawber for a careful reading of the manuscript. This work was supported by the Swiss National Science Foundation through the National Center of Competence in Research, "Materials with Novel Electronic Properties, MaNEP" and division II, New Energy and Industrial Technology Development Organization (NEDO) of Japan, and ESF (Thiox).

-
- * Now at Department of Physics and Astronomy, University of Aarhus, Ny Munkegade, Building 1520, DK-8000 Aarhus C; Electronic address: daniel@inano.dk
- [1] Y. J. Uemura *et al.*, Phys. Rev. Lett. **62**, 2317 (1989).
[2] T. Schneider and J. M. Singer *in Phase Transition Approach to High Temperature Superconductivity* (Imperial College Press, London, 2000).
[3] A. Hosseini *et al.*, Phys. Rev. Lett. **93**, 107003 (2004).
[4] D. M. Broun *et al.*, cond-mat/0509223.
[5] Y. Zuev *et al.*, Phys. Rev. Lett. **95**, 137002 (2005).
[6] T. Schneider, cond-mat/0509768.
[7] J. L. Tallon *et al.*, Phys. Rev. B **68**, 180501(R) (2003).
[8] C. C. Homes *et al.*, Nature **430**, 539 (2004).
[9] C. H. Ahn *et al.*, Nature **424**, 1015 (2003).
[10] D. Matthey *et al.*, Appl. Phys. Lett. **83**, 3758 (2003).
[11] J. Mannhart, Supercond. Sci. Technol. **9**, 49 (1996).
[12] H.-M. Christen *et al.*, Phys. Rev. B **49**, 12095 (1994), A. Bhattacharya *et al.*, Appl. Phys. Lett. **85**, 997 (2004).
[13] I. F. Herbut, Phys. Rev. B **61**, 14723 (2000).
[14] I. F. Herbut, Phys. Rev. Lett. **87**, 137004 (2001).
[15] In sample 1 is the factor of proportionality 1.9 times smaller
[16] K. Kim *et al.*, Phys. Rev. B **43**, 13583 (1991).
[17] Formula 2 is given in SI units.
[18] A. Walkenhorst *et al.*, Phys. Rev. Lett. **69**, 2709 (1992).
[19] T. T. M. Palstra *et al.*, Phys. Rev. B **41**, 6621 (1990).
[20] O. Brunner *et al.*, Phys. Rev. Lett. **67**, 1354 (1991).
[21] M. V. Feigel'man *et al.*, Phys. C **167**, 177 (1990).
[22] Ø Fischer *et al.*, Physica Scripta **T42**, 46 (1992).
[23] T. Schneider, *in The Physics of Superconductors* (edited by K. H. Bennemann and J. B. Ketterson, Springer, Berlin, 2004), p. 136.
[24] R. G. Goodrich *et al.*, Phys. Rev. B **56**, 14299 (1997).